Common-mode noise discrimination on multi-component seismic data

David C. Henley

ABSTRACT

In order to separate and/or attenuate noise contaminating seismic data, it is necessary to identify and use some characteristic of the noise which distinguishes it from "legitimate" seismic reflection energy. Sometimes, effective use of this characteristic requires the transformation of the input data samples to a new coordinate system via one or more transform or mapping operations. One unique characteristic available to analyze/separate certain noise modes on multi-component seismic data is that of particle motion polarization, since modes exhibiting characteristic polarization can be simultaneously and independently detected on sensors recording motion in two or more orthogonal directions.

One seismic noise mode well known for its distinctive polarization is the Rayleigh Wave or "ground roll", so it constitutes a good target for a noise attenuation algorithm based on some aspect of polarization. Another prominent example of strongly polarized noise is the ice flexural wave often encountered on seismic data recorded on floating ice in the arctic; it is also a prime candidate for some form of polarization filtering. A simple common-mode noise estimation technique was devised and applied to a multi-component field example of each of these two types of coherent noise. Based on our relatively simple tests, however, it appears that separation of coherent noise based on its polarization on two independent particle motion component wavefields is no more effective than estimation of the noise in each wavefield separately, based solely on the coherence characteristics of the noise.

INTRODUCTION

One of the fundamental ongoing problems in seismic data processing is the contamination of the desired reflection "signal" by coherent noise—seismic energy propagating in various wave modes that are not part of the backscattered reflection wavefield. Significant research in seismic data processing techniques has been devoted to studying the various modes that constitute coherent noise and to devising techniques for cancelling or attenuating them. Since the basic problem is that the noise interferes with the reflected wavefield in some fashion, all noise attenuation techniques share two features: they each attempt to isolate or separate the noise from the signal based on some distinguishing characteristic(s); and then they cancel, subtract, or otherwise filter out the noise based on those characteristics. If the noise has a well-behaved frequency spectrum, significantly different from that of signal, for example, it can be attenuated with a simple single-channel filter applied by convolution in the time domain or multiplication in the frequency domain. If, in addition, the noise is also correlated in some regular fashion over several channels, the pattern of this correlation can be used to further characterize the noise and assist in its separation.

The best known multi-channel noise attenuation technique involves the transformation of a seismic wavefield recorded on multiple adjacent channels to the 2-D Fourier domain, where signal and noise that are superimposed and entangled in the original XT domain are often well separated based on their localization in the f-k domain. Since coherent noise is often manifested at apparent velocities that differ significantly from those of reflection events; that noise can appear well isolated from signal in the f-k domain, where it can be attenuated by muting particular velocity-defined regions that contain predominantly coherent noise. Since this technique relies principally on velocity for separation of desired signal from noise, it loses its effectiveness when the velocity range inhabited by noise significantly overlaps that occupied by reflection, or when the noise mode exhibits a large amount of dispersion. A variation of the technique, rather than muting noise portions of the f-k domain to attenuate coherent noise instead mutes the signal to enhance or "model" the noise, then subtracts the inverse transformed noise in the XT domain. While these approaches are theoretically equivalent, numerical computation considerations often lead to one method outperforming the other. F-k techniques separate signal and noise based only on differences in their relative coherency patterns.

While f-k methods distinguish between signal and noise based mostly on their relative apparent velocities, a family of techniques based in the radial trace (RT) domain use both apparent velocity and apparent source point to isolate coherent noise and extract it from a recorded wavefield (Henley 1999, 2003). Because they use a data characteristic (apparent origin) in addition to apparent velocity, RT methods can often produce better separation of overlapping reflections and coherent energy with similar apparent velocities (for example, the long-offset limbs of shallow reflections contaminated by linear first arrivals and shallow refractions). In addition, the RT transform can very effectively capture dispersed coherent noise, since placing the RT origin at the apparent noise origin results in each frequency component of the dispersed noise being captured by a different radial trace, where it is monochromatic and thus easily modeled or cancelled (Henley 2004). Like the f-k methods, RT methods can either attenuate noise directly in the RT domain, or they can model the noise in that domain and subtract the modelled noise in the XT domain. RT methods, like f-k techniques, rely only on coherency pattern differences to separate signal and noise.

With multi-component data sets, an additional characteristic can be exploited for discriminating and separating some coherent noises. There are several well-known coherent noise modes which are known to involve particle motion in at least two dimensions; for example, the Rayleigh wave or "ground roll", and the ice flexural wave observed in floating ice plates in the arctic. For either of these modes the coherent noise will be recorded on at least two independent detector arrays, typically the vertical and inline horizontal particle motion detectors. If the relative phase of the particle motion between the two components is known, the coherent noise can be modelled by combining measurements from the two independent wavefield recordings (Kendall, et al. 2005). In the case of both ground roll and the ice wave, the phase relationships between vertical and inline (radial) particle motion are well known, as they are both elliptically polarized. This means that a 90 degree phase shift (plus or minus, depending upon which mode) will properly align events on one component wavefield with the same events on the other

wavefield for the purpose of estimating a mutual noise component. Several sophisticated methods have been described for the estimation of mutual noise (Kendall, et al. 2005), or for wavefield separation based on polarization (Diallo, et al. 2005), and (Samson and Olson, 1981). Some of these methods rely on an additional discrimination step that could be considered a part of the process—selective windowing of the noise on the input data, for example. We introduce here a relatively simple common-mode approach but make no claims as to its relative superiority with respect to other polarization methods.

COMMON-MODE NOISE ESTIMATION

The terminology for this technique comes from the assumption that the vertical and inline horizontal elements of a multi-component geophone will record two mostly independent wavefields, except for certain wave modes which exhibit coupled particle motion common to both. Since the vertical component elements capture mostly vertically travelling compressional wave particle motion and the inline component elements detect mostly vertically travelling shear wave particle motion, the vertical component shot gather will have few events in common with the inline horizontal one except for the common-mode noises, like ground roll and the ice wave, which have coupled particle motion in both dimensions. This means that the vertical and inline gathers will have some coherent noise events *in common,* except for phase. The goal, then, is to use the two independent components to obtain a joint estimate of the noise. A simple way to do this is to rotate the phase of the inline component to match that of the noise in the vertical component, to adjust the noise amplitude to match, and to average each pair of traces sharing the same geophone. Since most of the wavefield will be quite different on the two components (PP reflections on one, mainly phase-rotated PS converted waves on the other), it will tend to cancel while the coherent noise will add, being common between the two components.

In order to improve this common-mode noise estimate, we transformed it to the RT domain and applied a low pass filter to further attenuate residual reflection energy. This step is roughly equivalent to the guided derivation window used in other polarization filter implementations, since its purpose is to increase the relative isolation of signal and noise. It is this RT-enhanced common-mode noise estimate that is illustrated in our examples. It can be subtracted directly from the vertical component, but the phase rotation and any trace scaling must be reversed before subtracting it from the inline component. The phase rotations to be applied to the inline component are -90 degrees for ground roll (retrograde elliptical polarization), and +90 degrees for the coupled air wave. For the ice flexural wave -90 degrees is also appropriate. For seismic data containing more than one polarized mode with distinct polarizations, a separate common-mode estimate must be made for each.

EXAMPLES

Ground roll at Blackfoot

To test our common-mode polarization filter scheme on ground roll, we chose two shots from the much-studied Blackfoot 2-D 3C data set. The two shots are adjacent, but have significantly different S/N. In fact, the variability of the noise along the line argues against averaging the common-mode estimates over shots or receivers. Figure 1 is a

display of the vertical component traces for shot 73, while Figure 2 is its corresponding inline horizontal component trace gather. On this gather, the polarity of traces at negative offsets has been reversed, so that particle motion *away from* the shot is positive, and particle motion *toward* the shot is negative. Comparing the two gathers by eye, it can be seen that the pattern of ground roll is similar between the two, supporting the idea that a robust common-mode estimate is possible.
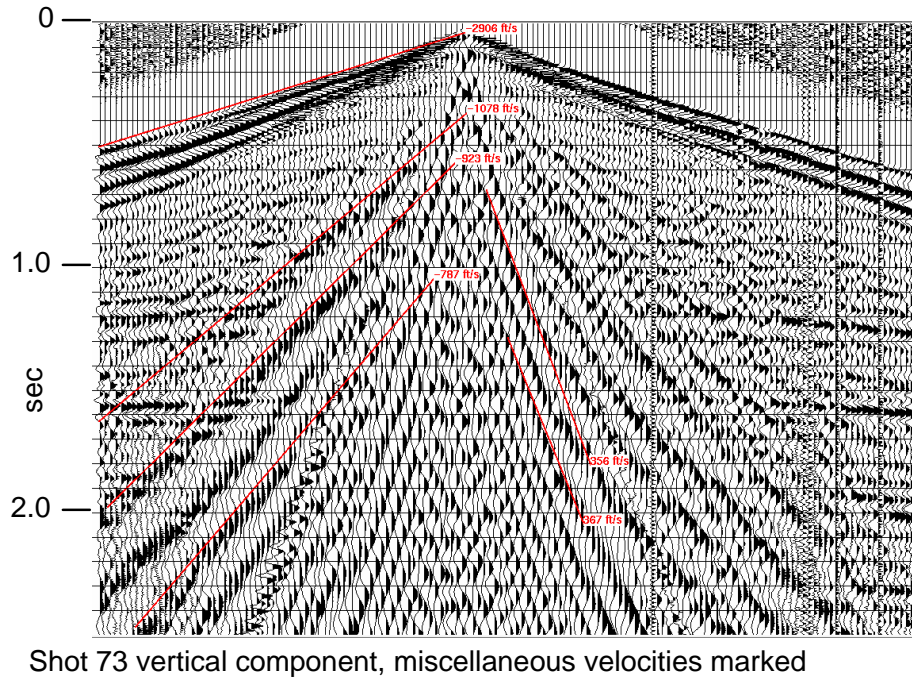

Shot 73 vertical component, miscellaneous velocities marked

FIG. 1. Vertical component shot gather 73 for Blackfoot 2D 3-C seismic survey. Various coherent noise velocities are marked.

Shot 73 inline horizontal component, miscellaneous velocities marked
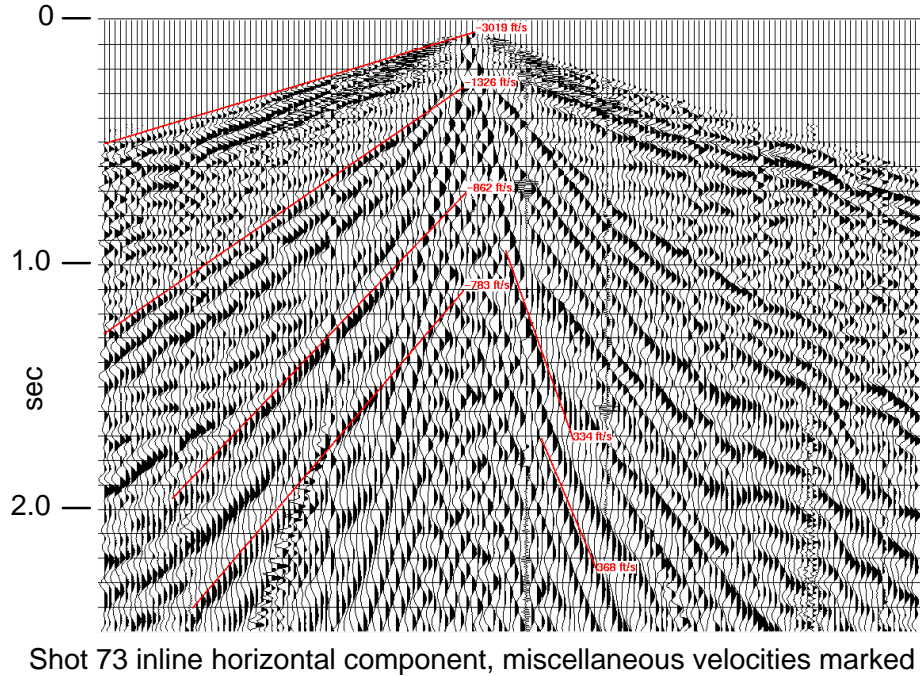
FIG. 2. Inline horizontal component shot gather 73 for Blackfoot 2D 3-C seismic survey. Various coherent noise velocities are marked.

To assist in the analysis of common modes, we created a display in which each pair of traces corresponds to the vertical and inline component at a single receiver. Thus, when corresponding events on each trace pair are horizontally aligned, we can be assured of their phase match. Their relative amplitudes can be readily judged from this display, as well. Figure 3 shows such a trace pair gather, in which no phase adjustment has been applied to the inline component. Close examination shows that the direct arrivals on the trace pairs are well-aligned, but neither the ground roll, nor the air-coupled waves are properly matched. In Figure 4, the trace pairs have been summed and displayed in colour contour to emphasize that the direct arrivals reinforce because of their phase alignment, but other modes do not. Figure 5 shows the trace pair gather for shot 73 after the inline traces have been phase-rotated by -90 degrees, and Figure 6 shows the summed and contoured gather. It is obvious from these displays that the ground roll has been aligned by this phase adjustment, the first step toward a common-mode estimate. Figures 7 and 8 are the corresponding trace pair and summed trace pair gathers when a phase rotation of +90 degrees has been applied to the inline component. From these displays, it can be seen that the air-coupled wave is now properly aligned and enhanced.
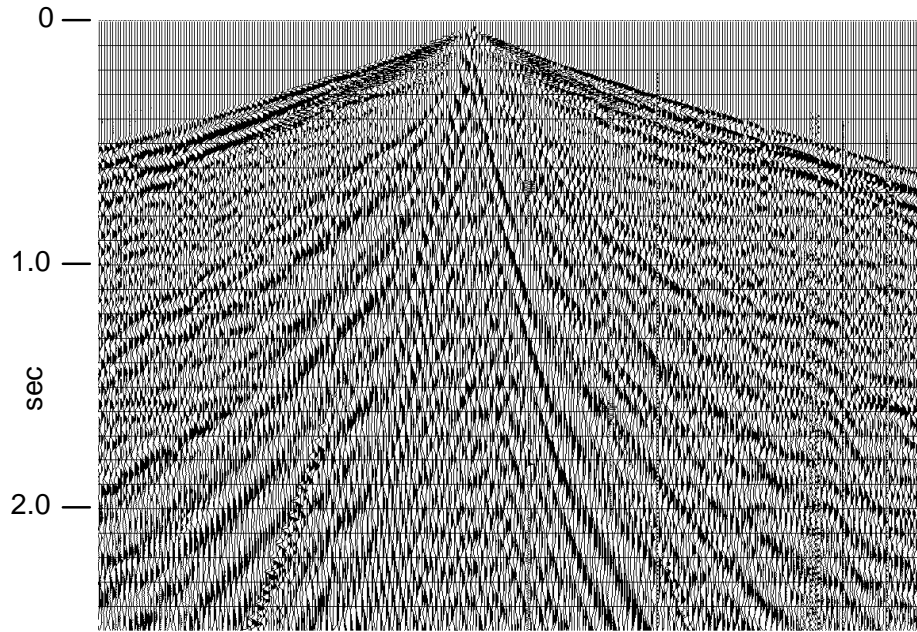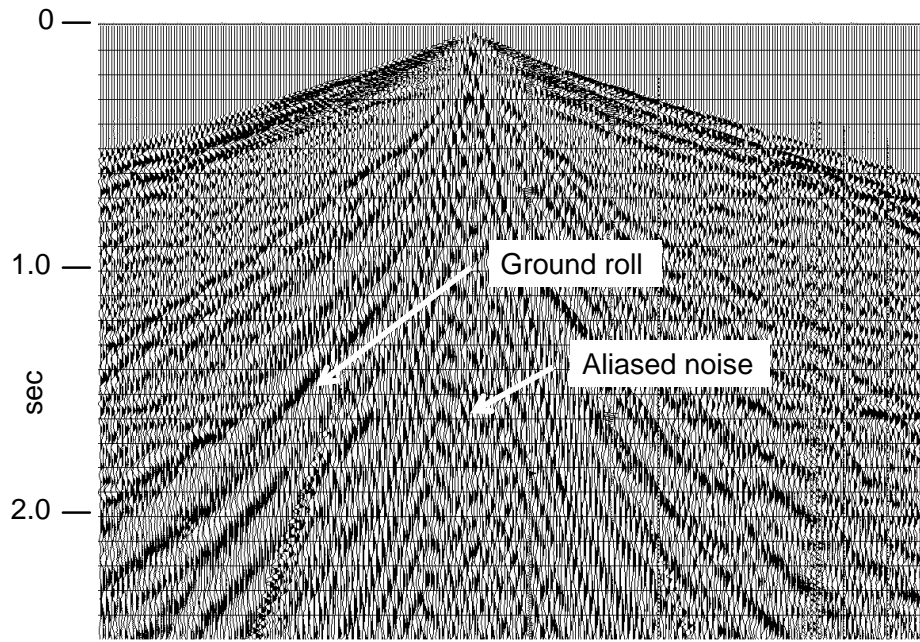
Shot 73 vertical and inline traces merged by pairs—no inline component phase adjustment—first arrivals aligned.

FIG. 3. Trace pair shot gather for Blackfoot shot 73. No phase adjustment has been applied to the inline component traces, so only the direct arrivals are aligned on the trace pairs.
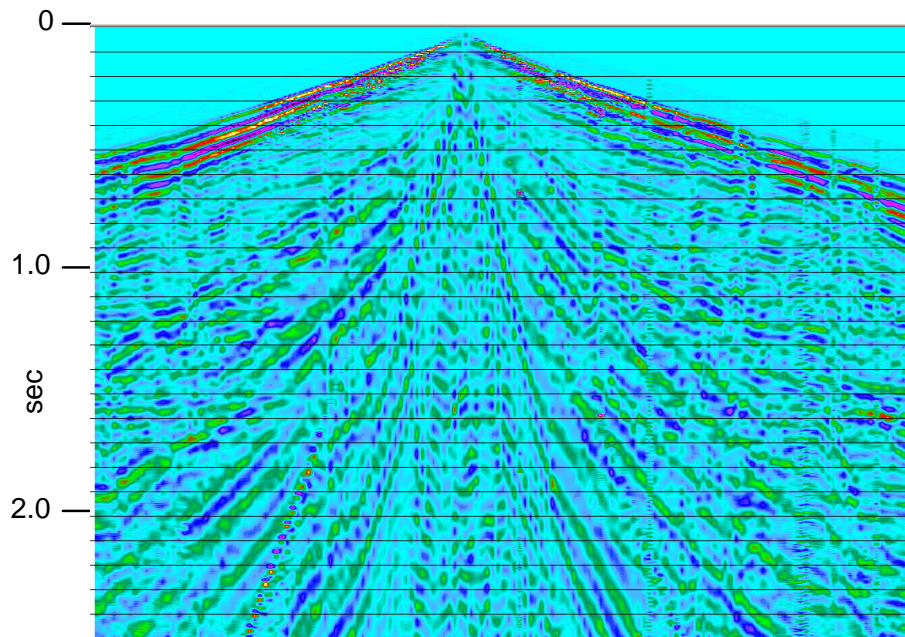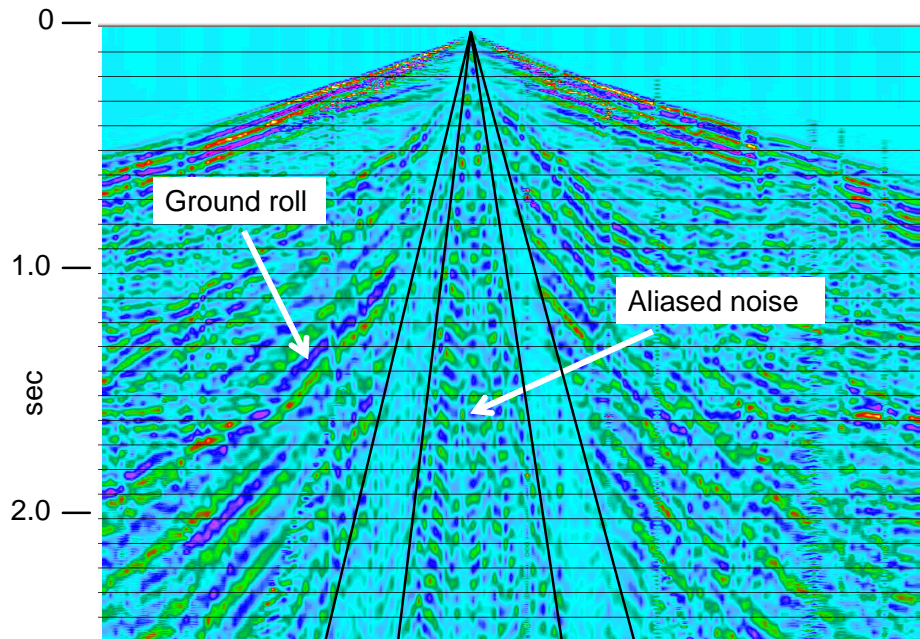

Shot 73 vertical and inline trace pairs summed—no inline component phase adjustment—first arrivals aligned

FIG. 4. Summed trace pairs—the "common mode" for Blackfoot shot 73 with no phase adjustment on the inline component traces. First arrivals and refractions are aligned and sum constructively.

Shot 73 vertical and inline traces merged by pairs—minus 90 degree inline component phase adjustment—ground roll and some aliased noise components now aligned.

FIG. 5. Trace pair gather for shot 73 with -90 degree phase rotation applied to inline component traces. Loops in the ground roll and the cone of aliased noise are now aligned.

Shot 73 summed inline and vertical trace pairs—minus 90 degree inline component phase adjustment—ground roll and aliased noise now aligned.

FIG. 6. Summed trace pairs—the "common mode" for shot 73 with the -90 degree phase rotation applied to the inline component traces. Ground roll and aliased noise components are much stronger than in Figure 4, although some early arrival energy still aligns strongly, as well. Note the two zones of cancelled energy separating the ground roll and aliased noise cone.
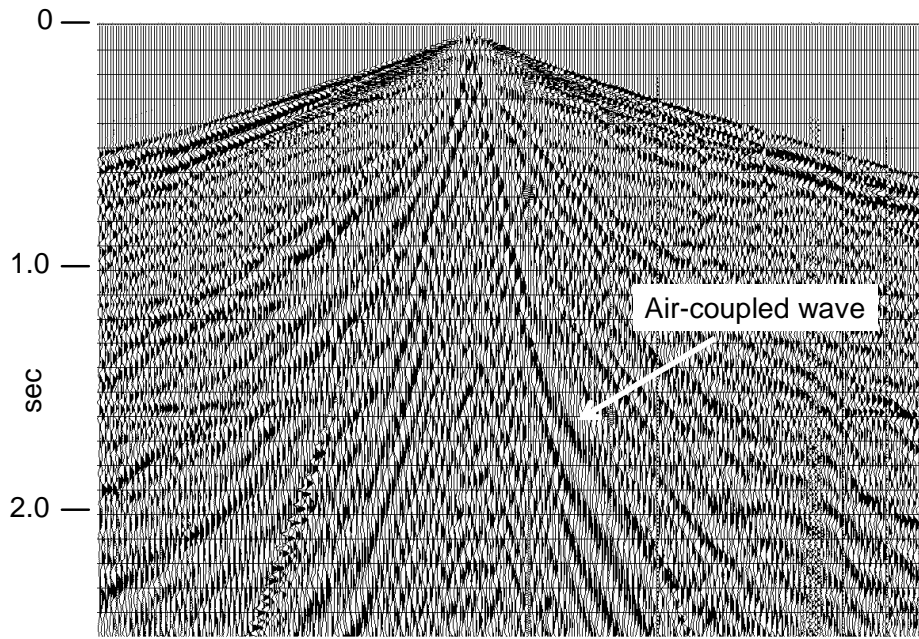
Shot 73 vertical and inline traces merged by pairs—plus 90 degree
inline component phase adjustment—air-coupled wave now aligned.

FIG. 7. Trace pair gather for shot 73 with a +90 degree phase rotation applied to the inline component traces. Much of the ground roll is now misaligned, but the air-coupled wave now appears well-aligned.
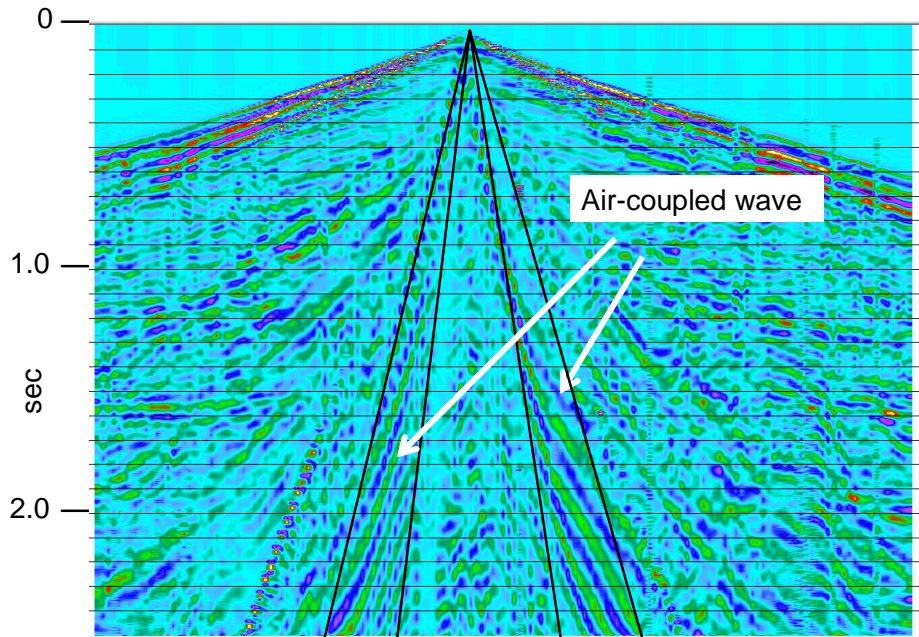

Shot 73 summed vertical and inline trace pairs—plus 90 degree inline
component phase alignment—air-coupled wave now aligned..

FIG. 8. Summed trace pairs for shot 73 with the +90 degree phase rotation applied to the inline component traces. While the energy in the ground roll and aliased noise cones is much diminished, the air-coupled wave is strong and fills the gaps apparent in Figure 6.

Since we're interested in making these noise estimates as robust as possible, we apply an RT low-pass filter (Henley 2003) in order to attenuate reflection signal as much as possible. We also want to remove as much coherent noise as possible, so we show the sum of the RT filtered ground roll and air-coupled wave estimates in Figure 9. The energy in this gather can be seen to be mostly coherent noise, although a low-frequency residual of the vertical reflection signal can also be seen. This residual could be eliminated by lowering the pass limits in the RT filter, however. In actual practice, we subtract the ground roll and air-coupled waves separately, since we have to apply a +90 degree phase shift to the ground roll estimate before subtracting it from the inline gather and a -90 phase shift to the air-coupled wave estimate before subtracting it from the inline gather.
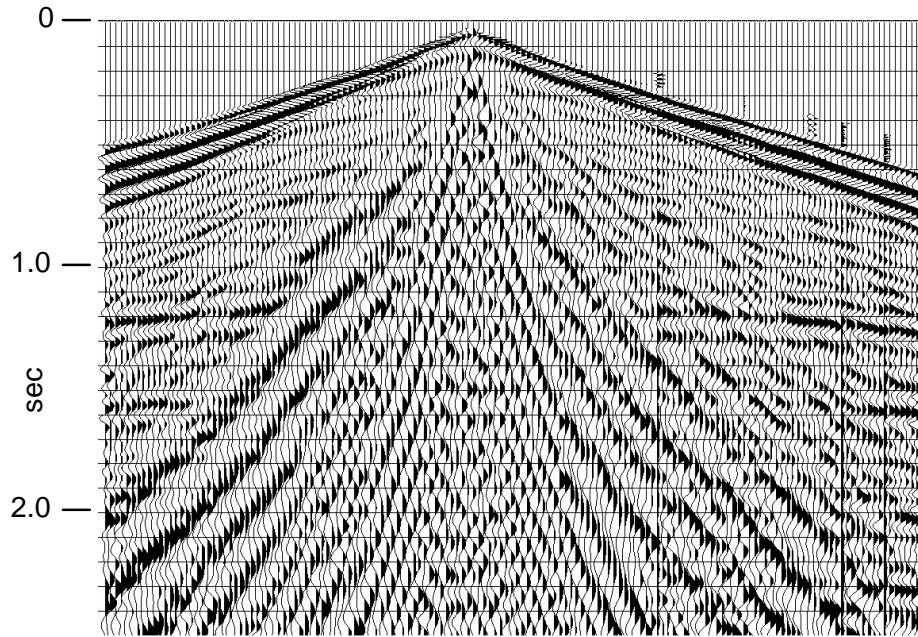

Shot 73 total common-mode noise

FIG. 9. The total "common-mode" noise estimate for shot 73. This estimate consists of a sum of the estimates for both -90 degree and +90 degree phase rotations of the inline component traces (Figures 6 and 8, respectively). Low frequency residual of the reflections could be reduced by lowering the pass band limits in the RT filter process.
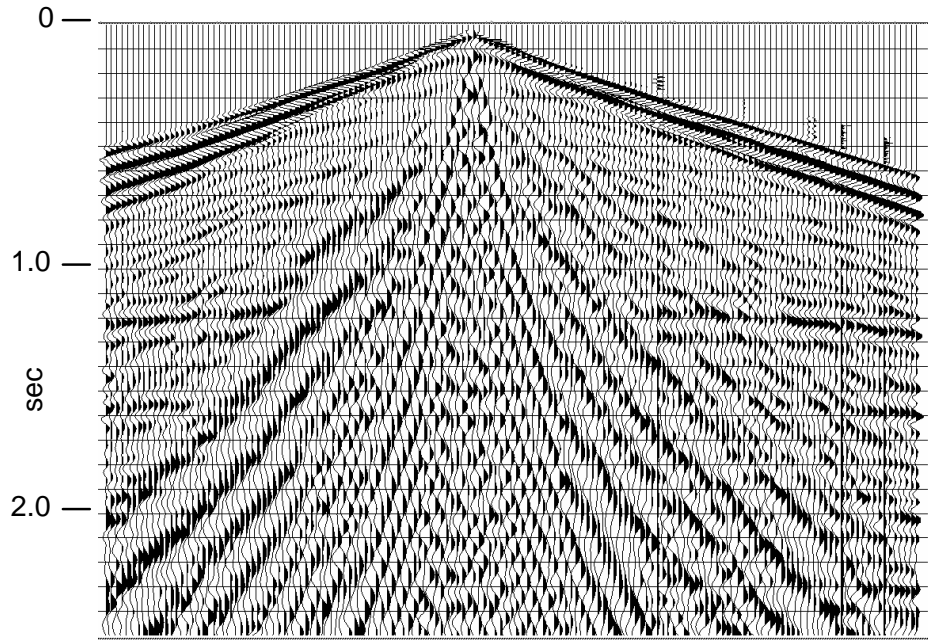
Shot 73 noise estimate from vertical component traces only

FIG. 10. Coherent noise estimated from only the vertical component shot gather for shot 73 using RT low-pass filtering.
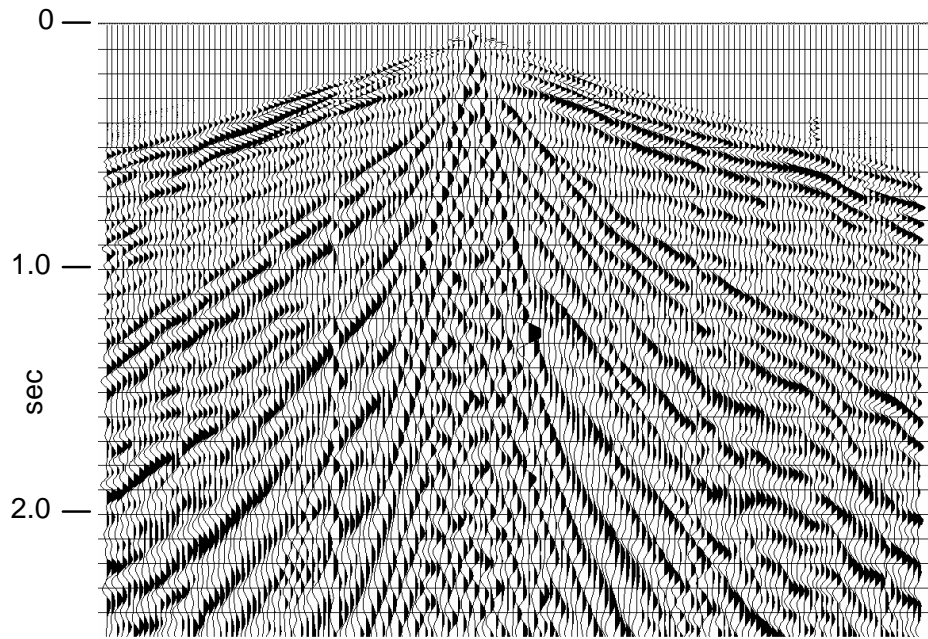
Shot 73 noise estimate from inline component traces only

FIG. 11. Coherent noise estimated from only the inline trace gather for shot 73 using RT low-pass filtering.

In the previous step, we described applying an RT low-pass filter to the common-mode noise estimates in order to further attenuate reflection energy from the noise estimates. To provide a suitable result for comparison to the common-mode subtraction scheme, we also computed an estimate of the total linearly coherent noise in the vertical component alone by applying the same RT low-pass filter to the raw vertical shot gather. That noise estimate is shown in Figure 10. Figure 11 shows the estimate of total linearly coherent noise in the inline gather, derived from the raw inline gather only. For neither of these noise estimates is polarization information used.

Shot 73 vertical component traces minus common-mode noise estimate.
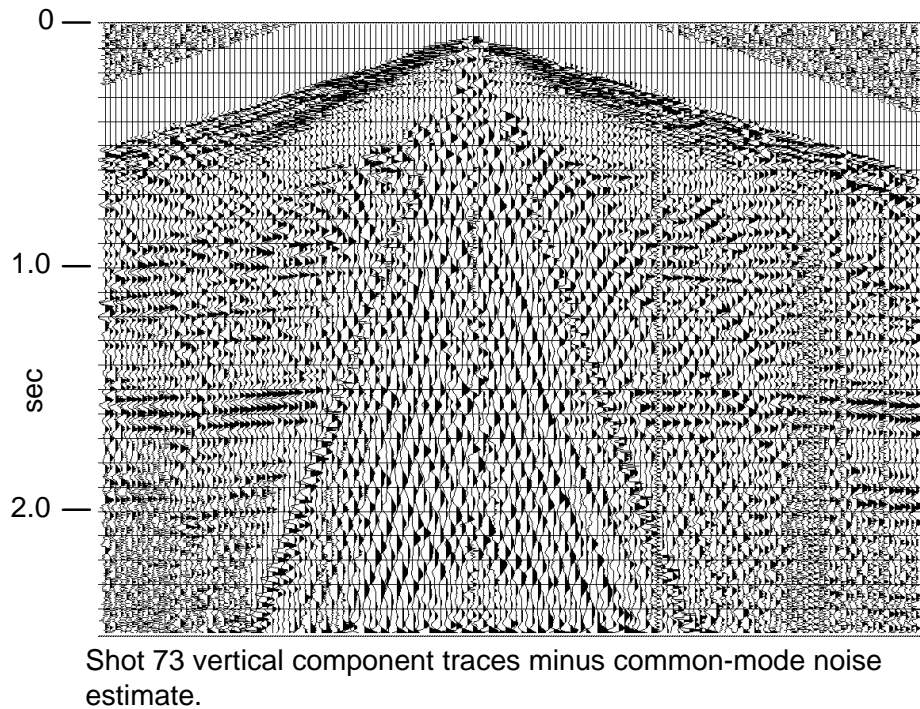
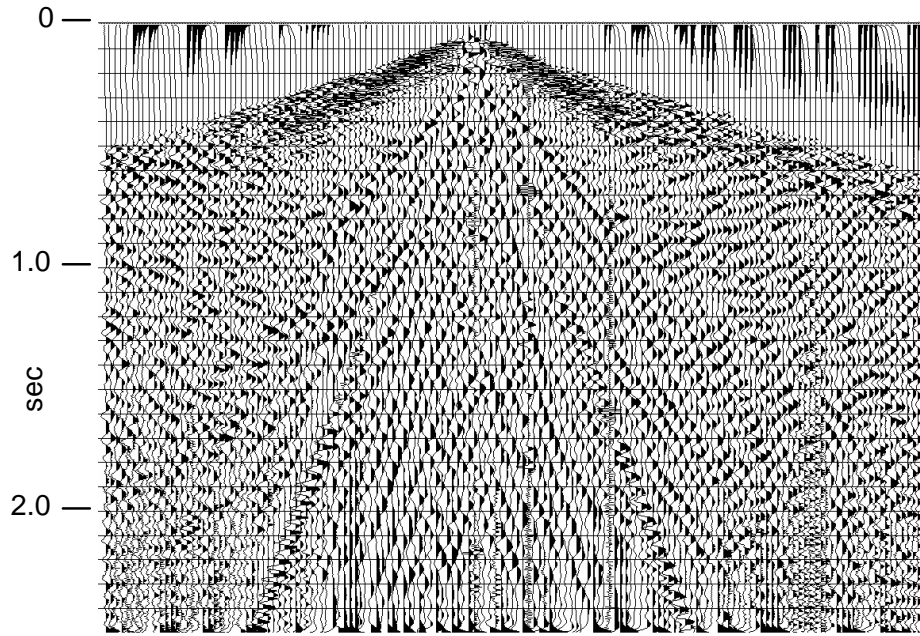FIG. 12. Vertical component shot gather for shot 73 with common-mode noise subtracted.
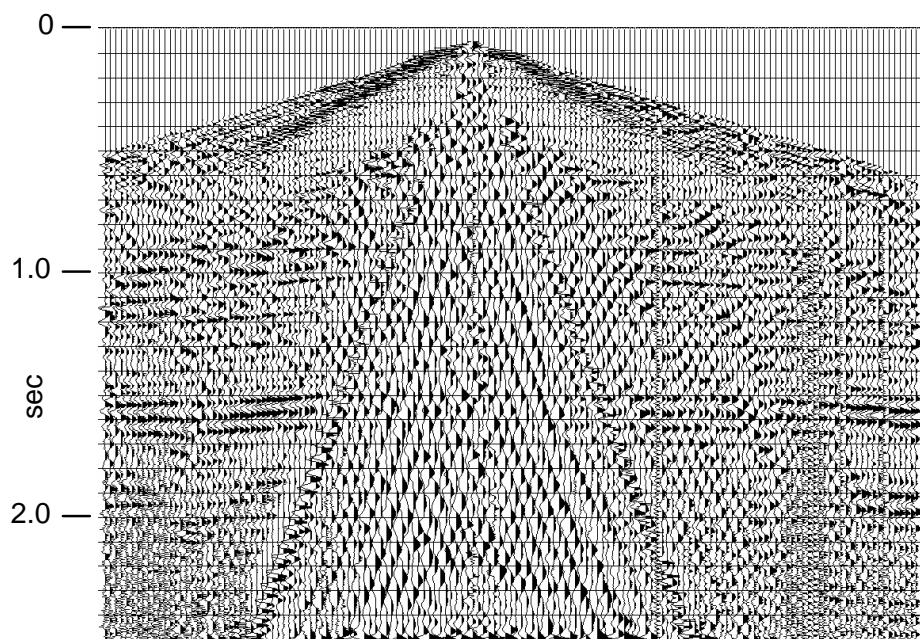
Shot 73 vertical component traces minus vertical component noise estimate.

FIG. 13. Vertical component shot gather for shot 73 with vertical component noise estimate subtracted. This result is very similar to that in Figure 12 except for improved removal of early arrival noise (which was not specifically targeted by the common-mode estimate.

Figure 12 is the vertical component gather for shot 73 with the total common-mode noise estimate subtracted, while Figure 13 shows this gather with the vertical coherent noise estimate (Figure 10) subtracted. As can be seen, the results are very similar—the reflection signal improvement being virtually the same in both cases. Close examination of the shallow portion of the gathers shows, however, that the vertical noise estimate is slightly superior to the common-mode noise estimate. The only way we could have made the results more comparable in this part of the record would be to make a third common-mode noise estimate, but with no phase shift to the inline traces, in order to estimate the common-mode direct arrival and refraction noise. Hence, we would have made three common-mode noise estimates, all to be subtracted from the input gather, in order to match the results of a single vertical component noise estimate.

Figure 14 shows the inline gather for shot 73 after subtraction of the common-mode noise estimates (with their proper phase rotations), while Figure 15 shows the same gather minus the inline noise estimate in Figure 11. For this gather, S/N is so low that the results are difficult to compare. We still note superior performance in the shallow part of the gather with the inline estimate, however, once again due to the better estimate of the direct arrivals by the simple RT low-pass filter.

Shot 73 inline component traces minus common-mode noise estimate.

FIG. 14. Inline component shot gather from shot 73 with common-mode noise estimate subtracted.
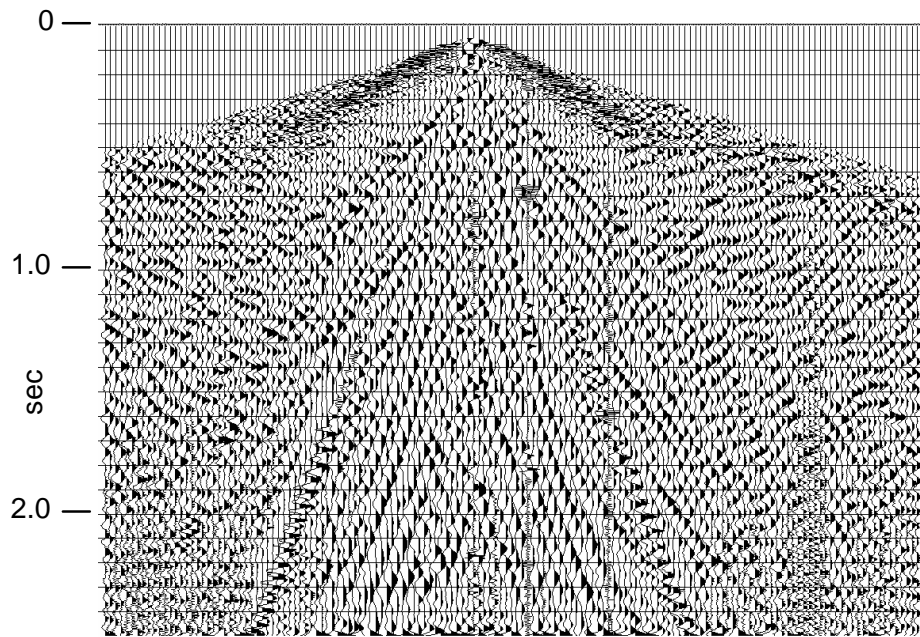
Shot 73 inline component traces minus inline component noise estimate.

FIG. 15. Inline component shot gather from shot 73 with inline noise estimate subtracted. This result does not differ much from that in Figure 14.

Shot 73 has a relatively low S/N compared with neighbouring shots, so we provide a similar comparison on shot 74 where the S/N is significantly improved. Figure 16 is the raw input vertical shot gather for shot 74, while Figure 17 is the corresponding inline gather. The total common-mode noise estimate is shown in Figure 18, while the corresponding vertical-only and inline-only noise estimates are shown in Figures 19 and 20, respectively.
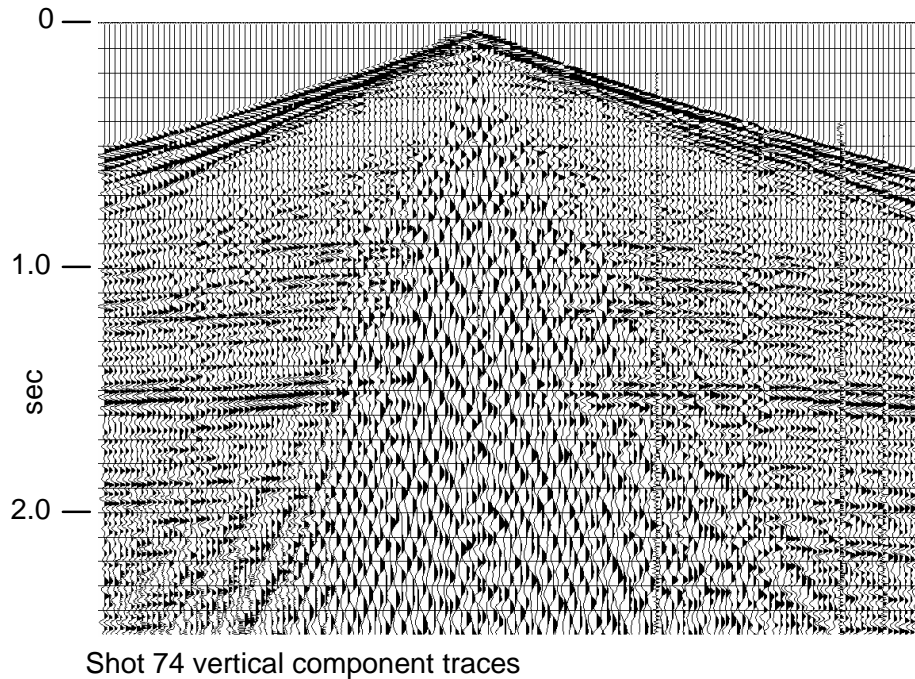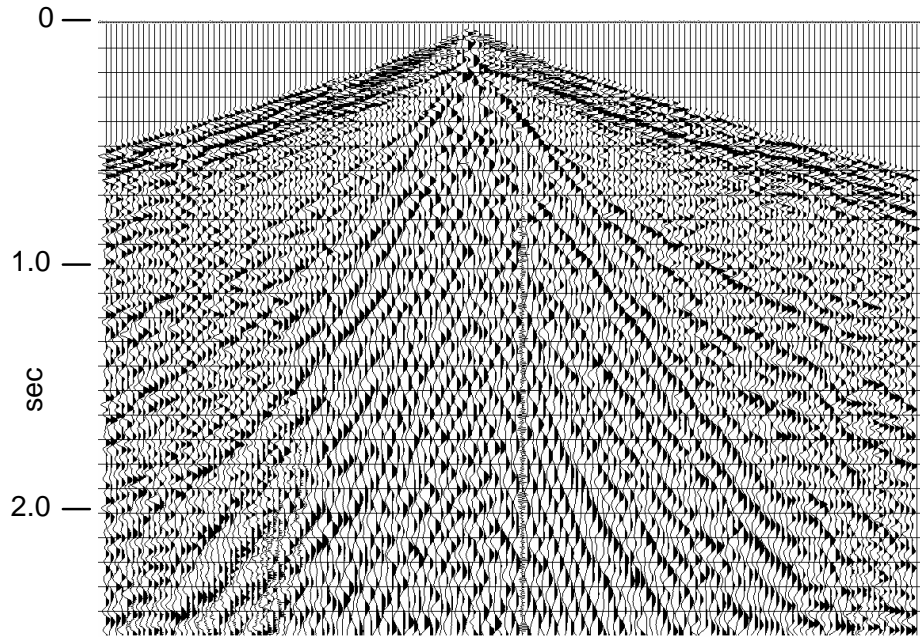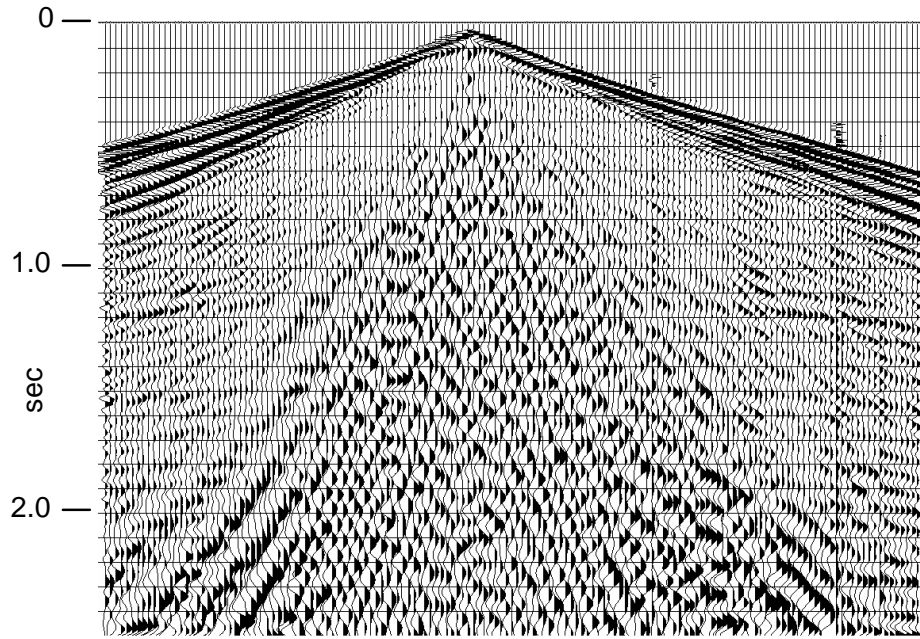

Shot 74 vertical component traces

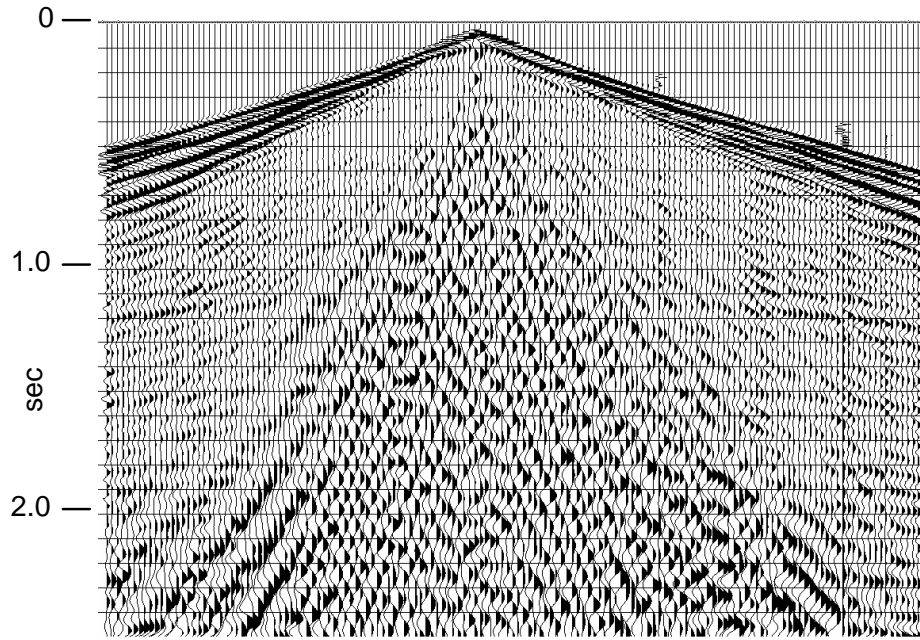FIG. 16. Vertical component shot gather for shot 74. S/N is much higher on this shot than on shot 73.

Shot 74 inline horizontal component traces

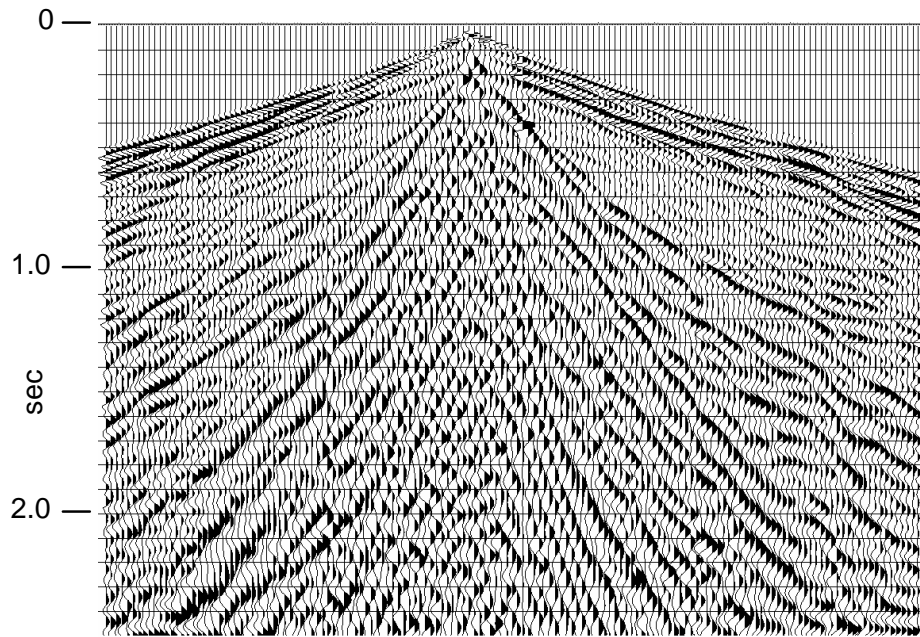FIG. 17. Inline horizontal component shot gather for shot 74.

Shot 74 common-mode noise estimate

FIG. 18. Common-mode noise estimate for shot 74, including both -90 degree and +90 degree inline component phase rotations.

Shot 74 vertical component noise estimate

FIG. 19. Coherent noise estimate obtained from only the vertical component traces using RT low-pass filtering.

Shot 74 inline horizontal component noise estimate

FIG. 20. Coherent noise estimate obtained from inline component traces only, using RT low-pass filtering.

Figure 21 is the vertical gather for shot 74 with the total common mode noise subtracted, and Figure 22 is the same gather with the vertical-only noise estimate subtracted. For this gather, the common-mode results are clearly inferior. Figures 23 and 24 show the comparable results for the inline component; and here, as well, the common-mode results are clearly inferior. In this case, faint reflections can be seen on the gather with subtracted inline-only noise estimate; but nothing appears on the gather with subtracted common-mode noise estimate.

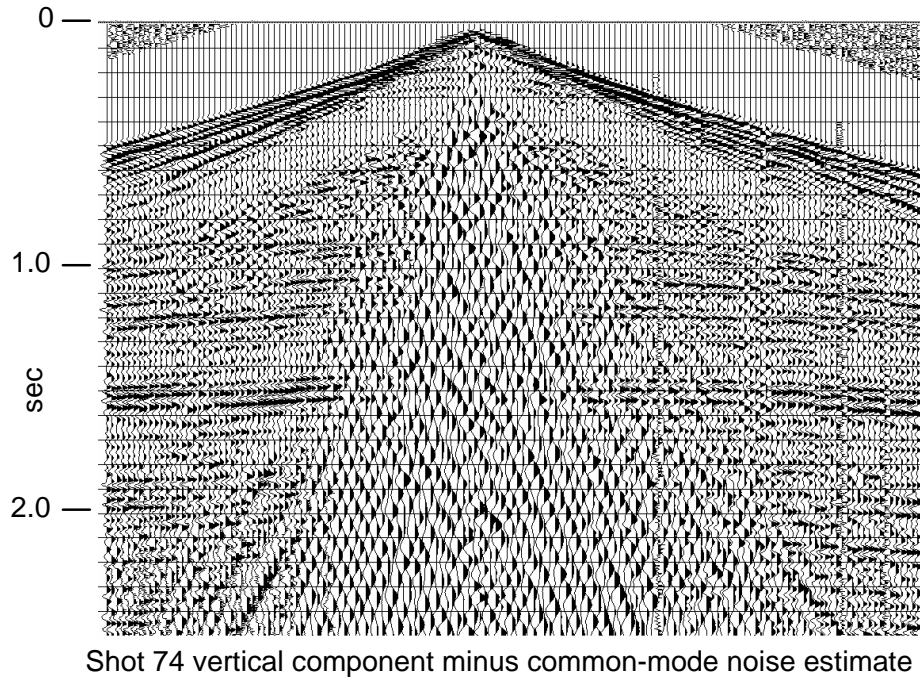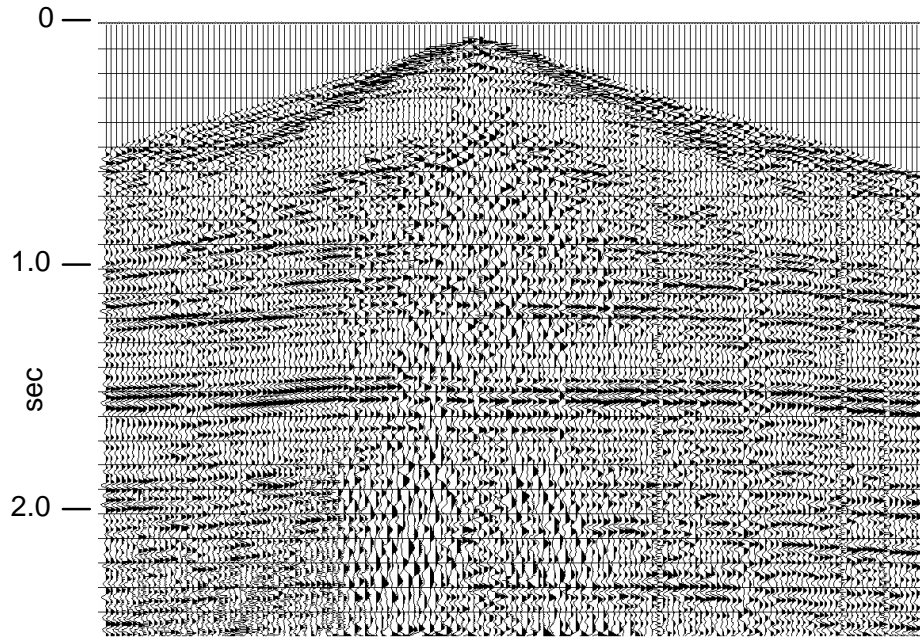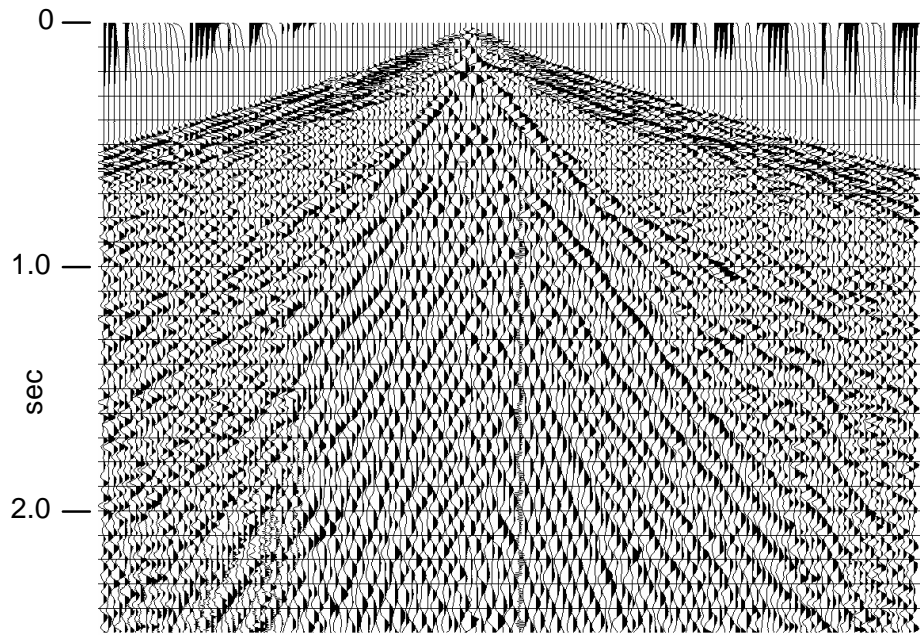Shot 74 vertical component minus common-mode noise estimate

FIG. 21. Shot 74 vertical component gather with common-mode noise estimate subtracted.

Shot 74 vertical component minus vertical noise estimate

FIG. 22. Shot 74 vertical component gather with vertical component noise estimate subtracted. Note the significant improvement over the results in Figure 21.

Shot 74 inline horizontal component minus common-mode noise estimate

FIG. 23. Shot 74 inline component gather with common-mode noise estimate subtracted.
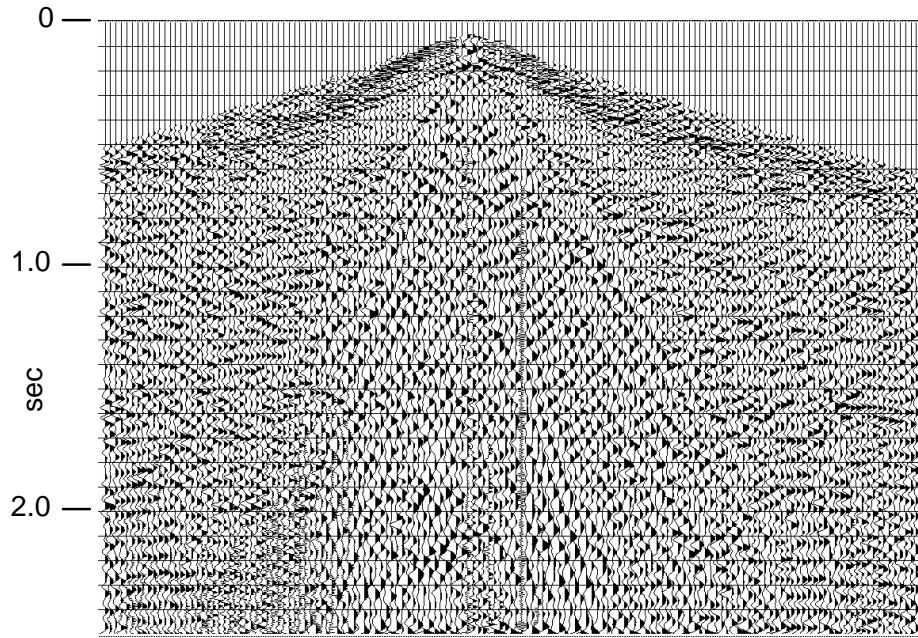
Shot 74 inline horizontal component minus inline noise estimate

FIG. 24. Shot 74 inline component gather with inline coherent noise estimate subtracted. The appearance of faint reflections indicates the superiority of this noise estimate.

To summarize the Blackfoot results: there is no evidence that common-mode noise estimates made using two components of particle motion offer any advantage over estimates of total linearly coherent noise made on each component separately. In fact, it requires at least three separate common-mode noise estimates to address the coherent noise that is estimated in one pass of regular RT domain noise modelling. More emphatically, since we used exactly the same RT domain low-pass filter to enhance the wavefield separation for the common-mode estimates, we can only conclude that for the Blackfoot data, merging information from the two components degrades the estimate of either one. Likewise, averaging noise estimates over two or more shot gathers would likely degrade the common-mode estimate even further, due to the spatial variability of the coherent noise.

Hansen Harbour—ice flexural wave

Another example of a coherent noise mode for which vertical and horizontal inline motion are strongly polarized is the ice flexural wave observed when recording seismic data on floating ice in artic regions (Ewing et al., 1957). This particular noise mode is one of the strongest known; and when the seismic source and receivers are both placed on the ice surface, the noise typically overwhelms signal by as much as 80 dB. In some cases, the dynamic range of the recording system is insufficient to allow recovery of the reflection signal even when the noise is strongly attenuated. The ice flexural wave is also often highly dispersed, with velocities ranging from well below air velocity to ice compressional velocity at 3000 m/s, so that ice wave contamination often covers an entire trace gather. Because of its strength and coherence, this noise should provide an ideal test of common-mode noise removal.

Figure 25 shows two vertical component shot gathers from the Hansen Harbour area of the MacKenzie Delta. The gathers are unscaled to show the relative strength of the ice wave compared to all other energy on the gather. For this survey, the 3-C geophone spread straddles the shoreline, with the left half on floating ice and the right half on solid land. The source was a vertical vibrator located off the left end of the spread, on the floating ice. Figure 26 is the same pair of gathers after application of AGC. From these figures the strength and dispersion of the ice wave can both be seen.

Vertical component shot gathers from Hansen Harbour 3-C
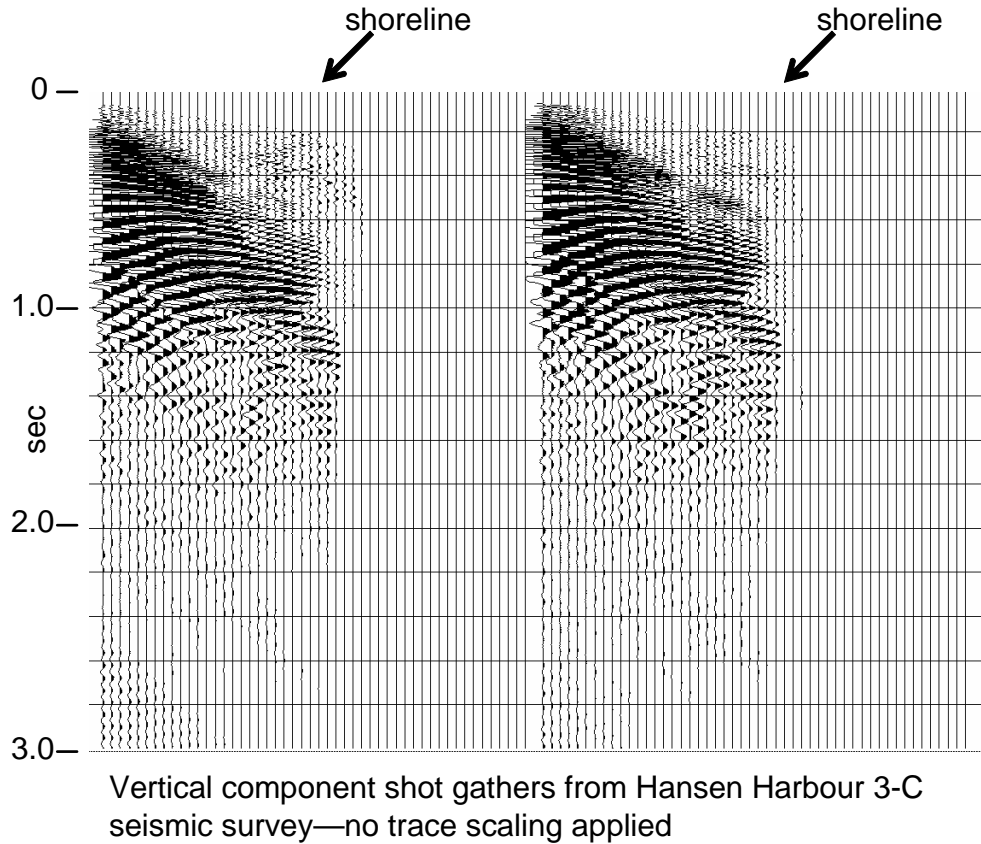seismic survey—no trace scaling applied

FIG. 25. Two vertical component shot gathers from the Hansen Harbour 2D 3-C seismic survey. The traces have not been scaled, in order to show the strength of the ice flexural wave noise.

Vertical component shot gathers from Hansen Harbour 3-C
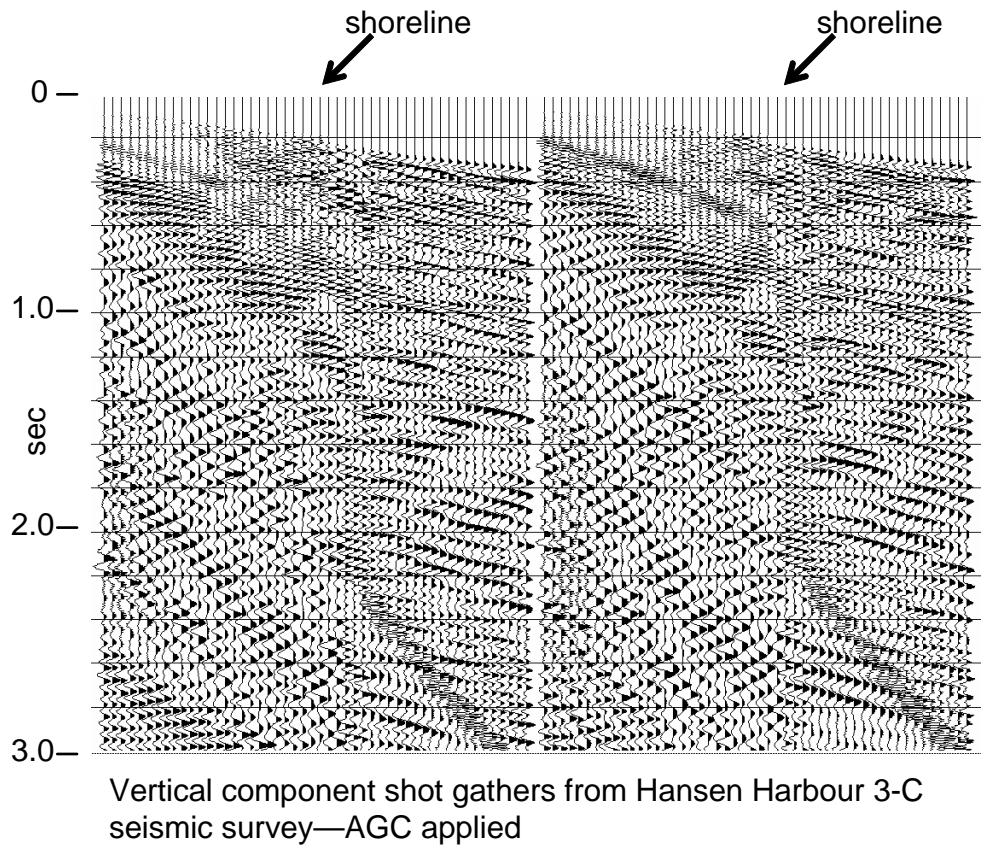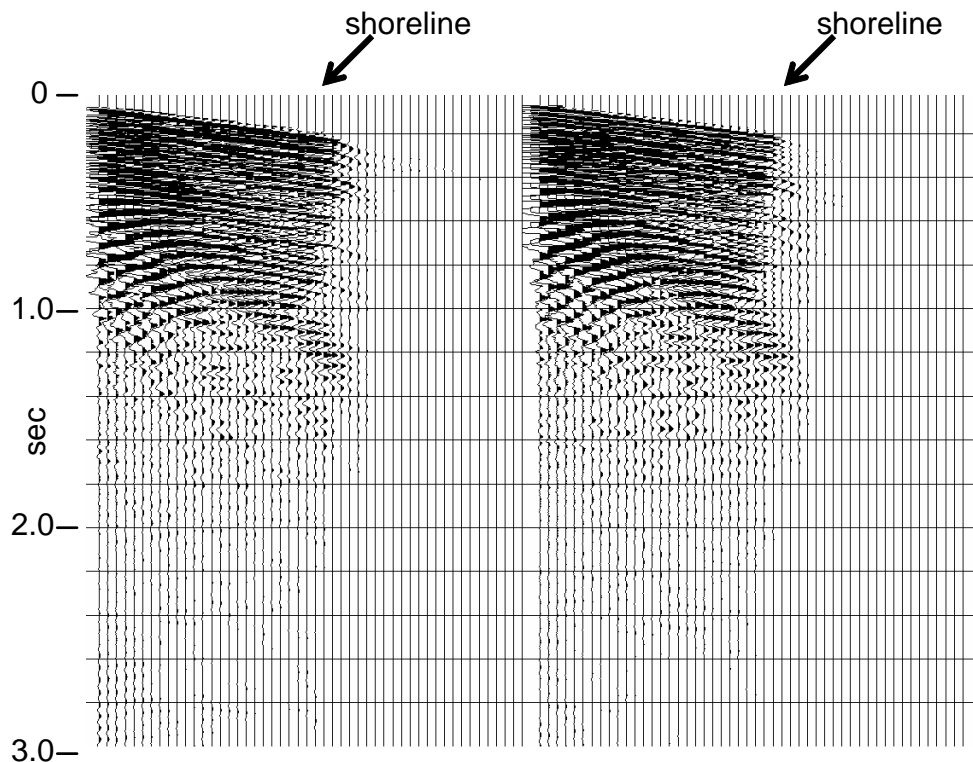seismic survey—AGC applied

FIG. 26. Vertical component shot gathers from Hansen Harbour after AGC, in order to show the rest of the wavefield, much of which is also coherent noise.

The corresponding inline shot gathers are shown in Figures 27 and 28; where it can be seen that the ice wave appears very similar in strength and appearance to that recorded on the vertical component phones.

Inline horizontal component shot gathers from Hansen
Harbour 3-C seismic survey—no trace scaling applied

FIG. 27. Inline horizontal component shot gathers from Hansen Harbour. Traces are unscaled to show the relative strength of the ice flexural wave.

Inline horizontal component shot gathers from Hansen
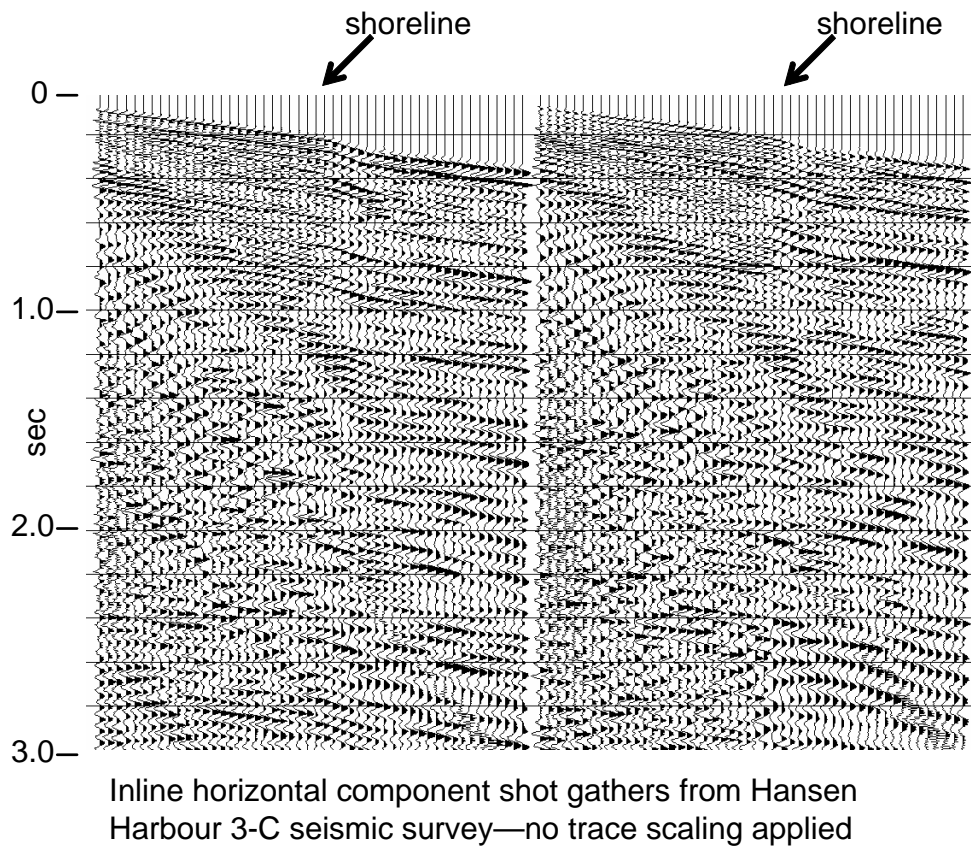Harbour 3-C seismic survey—no trace scaling applied

FIG. 28. Inline horizontal shot gathers from Hansen Harbour with AGC applied to show the rest of the wavefield, much of which is coherent noise.

In order to apply our common-mode technique to these data, we first formed trace pair gathers as shown in Figure 29. To confirm the polarization of the inline component with respect to the vertical component, we show Figures 30 and 31, with +90 degrees and -90 degrees phase shift applied to the inline traces, respectively. These figures make it clear that -90 degrees correctly aligns the vertical and inline ice wave components. The common mode ice wave estimate is computed as before by summing the trace pairs, then applying a radial trace domain low-pass filter to attenuate any residual PP or PS reflection energy. As part of an ice wave attenuation procedure described by Henley (2004), Gabor deconvolution (Margrave and Lamoureux, 2001) is applied to a shot gather after subtraction of the estimated noise in order to enhance reflection signal energy.

Trace pair shot gathers from Hansen Harbour 3-C seismic
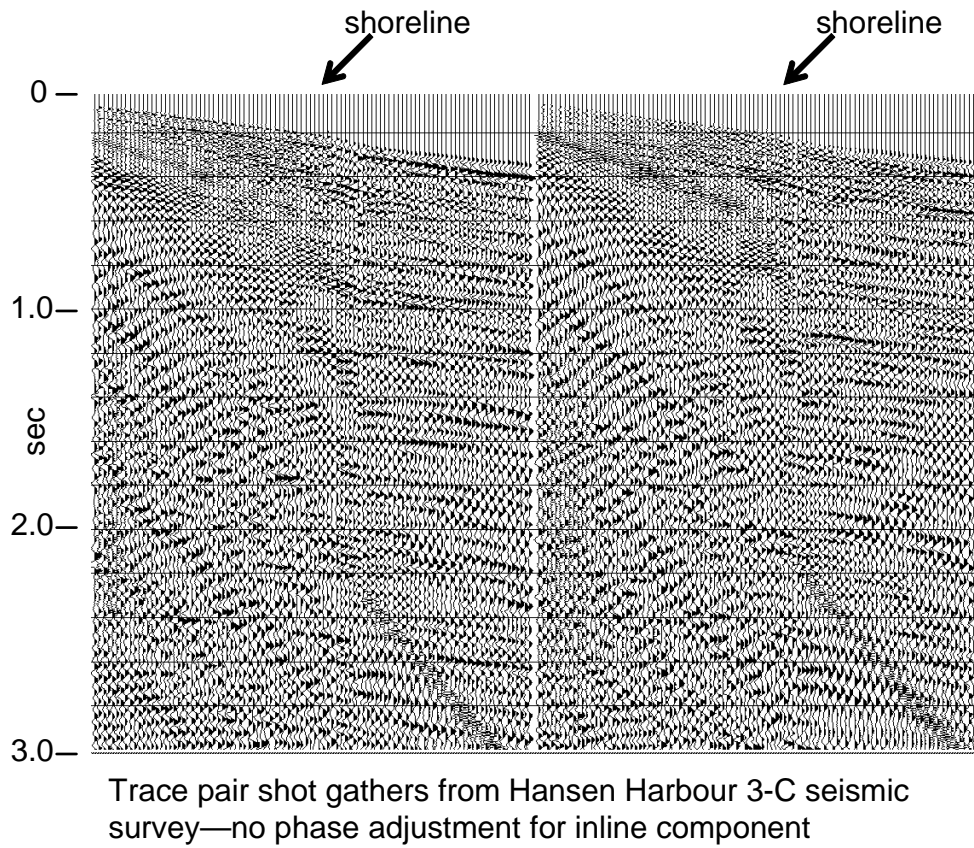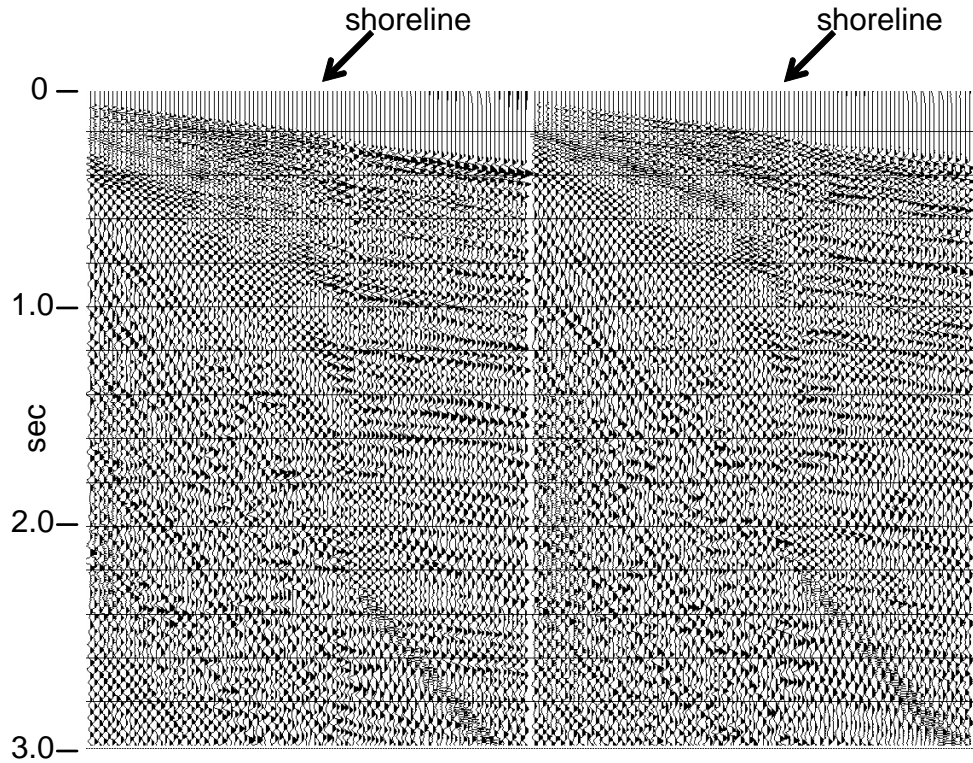survey—no phase adjustment for inline component

FIG. 29. Trace pair shot gathers for Hansen Harbour shots with no phase rotation applied to the inline traces.

Trace pair shot gathers from Hansen Harbour 3-C seismic survey—
plus 90 degree phase adjustment for inline component

FIG. 30. Trace pair gathers with +90 degree phase rotation applied to the inline component traces. Almost nothing aligns using this phase orientation.

Trace pair shot gathers from Hansen Harbour 3-C seismic
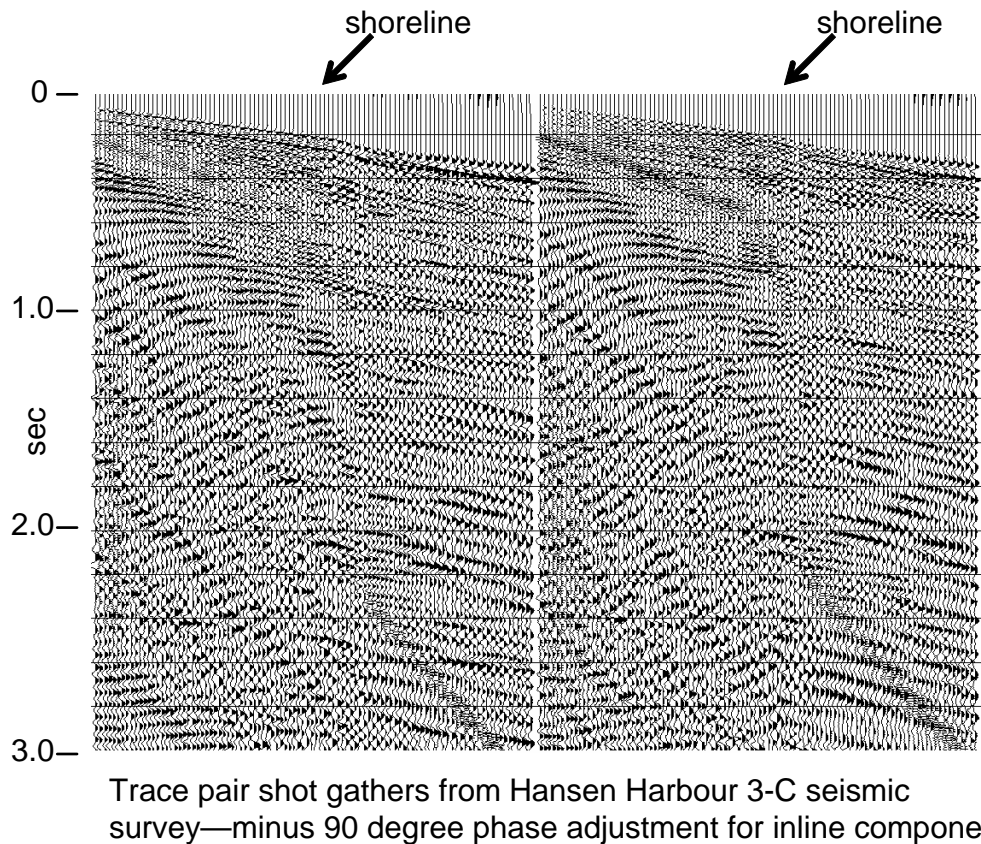survey—minus 90 degree phase adjustment for inline component

FIG. 31. Trace pair shot gathers with -90 degree phase rotation applied to the inline component traces. The ice flexural modes, as well as some of the other linear modes show good alignment.

The common-mode noise estimate is shown in Figure 32. Note that in addition to the ice wave, a number of apparently linear modes on the land-fast side of the spread are represented in the estimate. Figure 33 shows the original gathers from Figure 26 with no explicit ice wave suppression applied, but only Gabor deconvolution, to attempt to enhance reflection signal with respect to noise by spectral whitening. In Figure 34, the common-mode ice wave estimate has been subtracted from the gathers before deconvolution. For further comparison, Figure 35 shows the same gathers after spectral clipping in the radial trace domain followed by Gabor deconvolution in the XT domain, the procedure described by Henley (2004). While Figure 34 shows clear improvement over Figure 33, it is apparent that some residual ice wave and other linear energy remains, and there are no particular signs of spatially coherent underlying reflections. In Figure 35, however, most of the ice wave is gone, as is most of the linear noise at long offsets and times. Fragmentary reflections are visible on these gathers. Results for the inline horizontal component are not shown here, but are comparable.
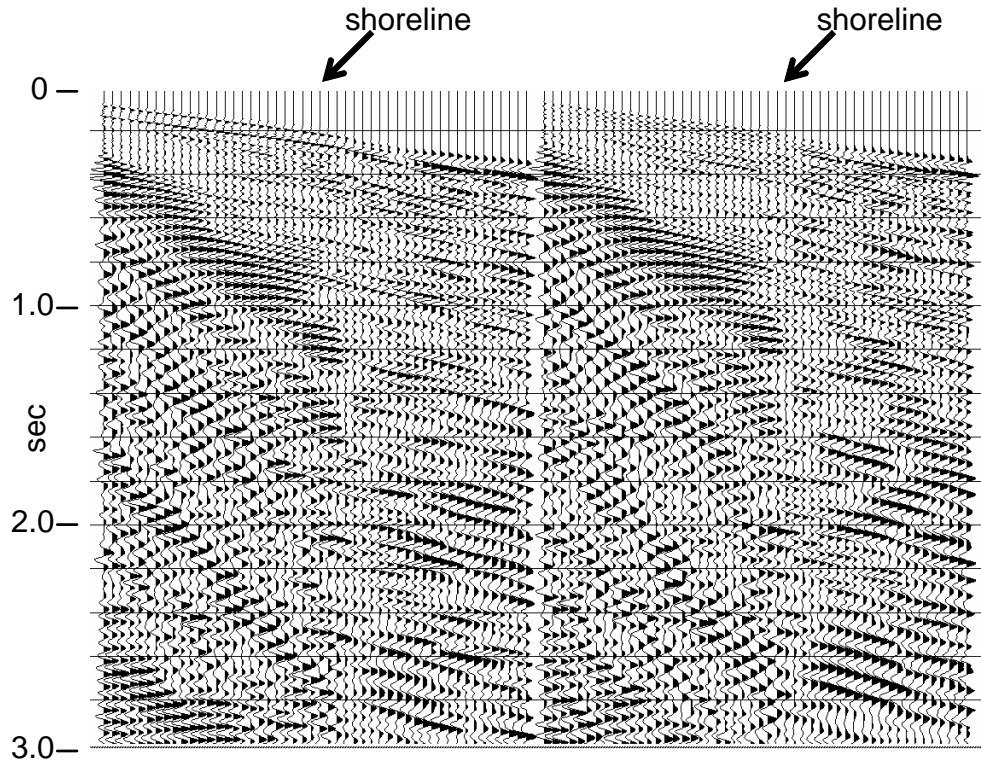
Common-mode noise estimate using vertical/inline trace pairs with
-90 degree inline phase adjustment

FIG. 32. Common-mode noise estimate created by applying RT low-pass filtering to the summed trace pairs from Figure 31. Note that some linear noise is estimated in addition to the ice flexural modes.

Gabor deconvolution applied to raw vertical component shot gathers to boost reflection signal
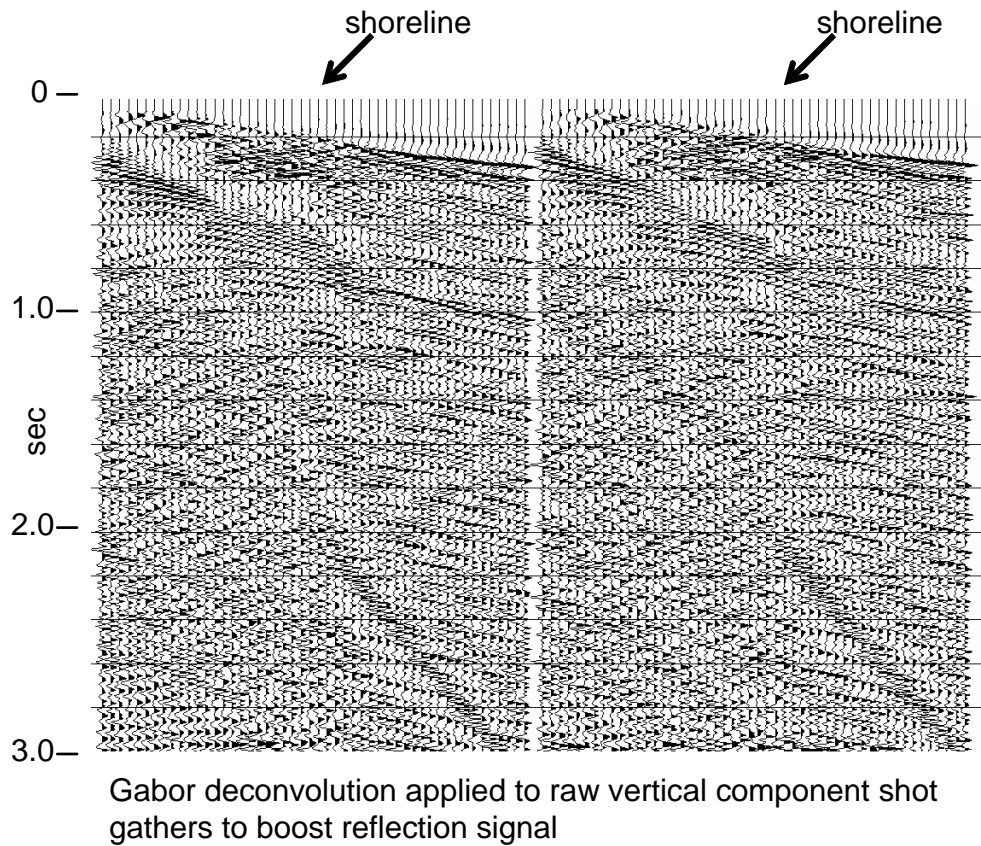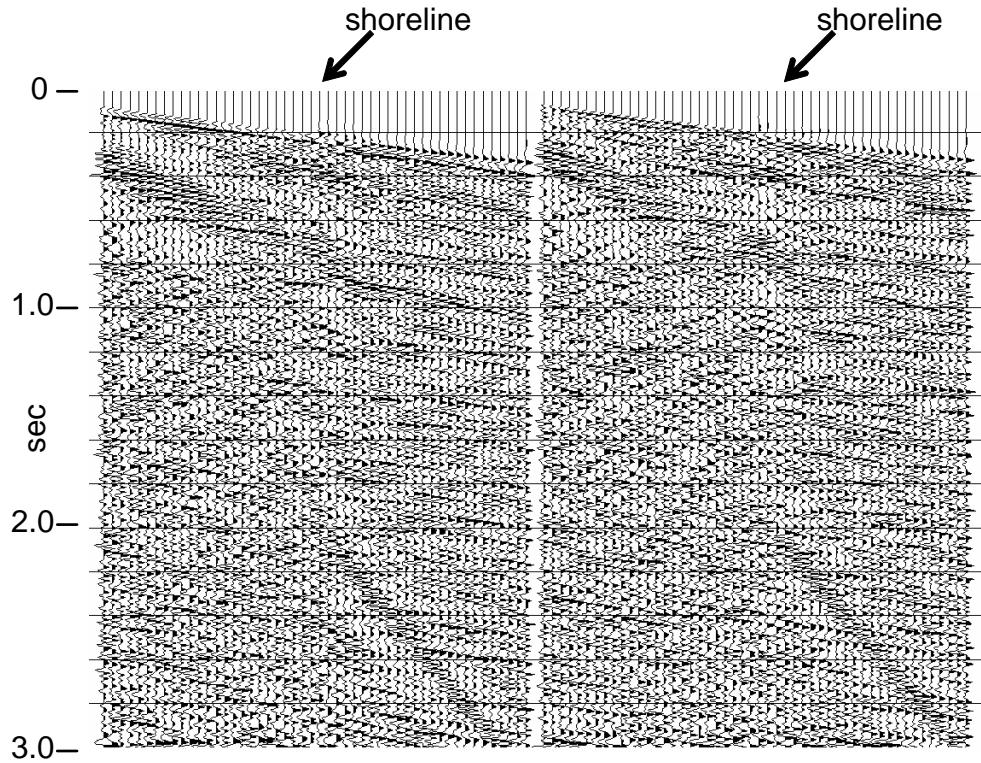
FIG. 33. An attempt to remove the ice flexural wave modes simply by applying non-stationary (Gabor) deconvolution to the shot gathers. While the modes are reduced, there is little evidence of underlying reflection energy.

Gabor deconvolution applied to vertical component shot gathers
after subtraction of common-mode noise estimate in Figure 33.

FIG. 34. Common-mode noise in Figure 32 subtracted from vertical component shot gathers before application of non-stationary deconvolution. More noise is removed than in Figure 33, but there is still little evidence of reflection energy.
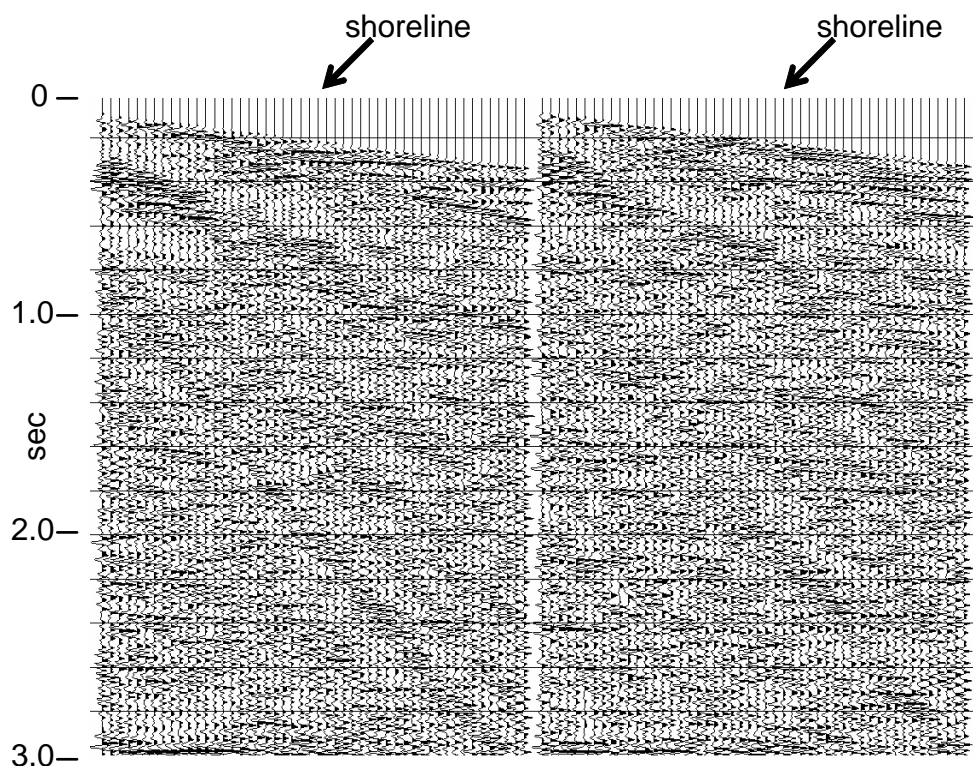
Gabor deconvolution applied to vertical component shot gathers after RT domain spectral clipping. Fragmentary reflections are visible.

FIG. 35. Rather than estimating and subtracting noise modes from the shot gathers, these gathers have been transformed to the RT domain, where spectral peaks due to the ice flexural modes and other coherent noise have been "clipped", a non-linear procedure. Non-stationary deconvolution finishes the noise removal process. Fragments of underlying reflections are now visible on these shot gathers.

These results indicate that even with strongly correlated vertical and inline horizontal components, subtraction of ice wave and other linear noise estimated by our common-mode method is less effective than a technique which separates the highly dispersed ice wave by origin, velocity, and monochromatic frequency (Henley 2004) on single component shot gathers.

CONCLUSIONS

The concept of using particle motion polarization to discriminate against particular wave modes on multi-component seismic data can be used to reduce some kinds of coherent noise on these data. One way of implementing such a noise reduction scheme is by using knowledge of the polarization for a particular noise mode to match the phase of the vertical and inline components of the noise and to sum them to get a so-called "common-mode" noise estimate. This can then be subtracted from the original vertical data, and phase-rotated and subtracted from the inline data. In a trial of this method, it proved to be less effective in estimating the noise than radial trace domain techniques applied to the individual vertical and inline components. The RT techniques, which rely on the apparent velocity and point of origin of coherent noise, do not require the noise to

fit a particular polarization model and hence can attenuate all linear modes simultaneously. Even when assisted by RT techniques to improve its noise discrimination, the common-mode polarization method showed no advantage.

ACKNOWLEDGEMENTS

REFERENCES

Diallo, M.S., Kulesh, M., Holschneider, M., and Scherbaum, F., 2005, Instantaneous polarization attributes in the time-frequency domain and wavefield separation: Geophysical Prospecting, **53**, No. 5, pp 723-732.

Ewing, W.M., Jardetzky, W.W., and Press, F., 1957, Elastic waves in layered media, McGraw-Hill, pp281-327.

Henley, D.C., 1999, The radial trace transform: an effective domain for coherent noise attenuation and wavefield separation: 69th Ann. Int. Mtg., Soc. Expl. Geophys., Expanded Abstracts, 1204-1207.

Henley, D.C., 2003, Coherent noise attenuation in the radial trace domain: Geophysics, **68**, No. 4, pp 1408-1416.

Henley, D.C., 2004, Attenuating the ice flexural wave on arctic seismic data: CREWES 2004 research report vol. **16**.

Kendall, R., and De Meersman, Kristof, 2005, A complex SVD-polarization filter for ground roll attenuation on multicomponent data: 2005 CSEG annual convention, Expanded Abstracts.

Margrave, G.F., and Lamoureux, M.P., 2001, Gabor deconvolution: CREWES 2001 research report, vol. **13**.

Samson, J.C. and Olson, J.V., 1981, Data-adaptive polarization filters for multichannel geophysical data: Geophysics, **46**, No. 10, pp 1423-1431.